Desalination and Water Treatment
www.deswater.com
doi: 10.1080/19443994.2013.800003

52 (2014) 2241–2252
February

Taylor & Francis
Taylor & Francis Group

Adsorptive removal of humic acid on activated carbon prepared from almond shell: approach for the treatment of industrial phosphoric acid solution

Abdessalem Omri[a,*], Mourad Benzina[a], Wassim Trabelsi[b], Najwa Ammar[b]

[a]*Laboratory of Water Energy Environment (LR3E), code: AD-10-02, National School of Engineers of Sfax, University of Sfax, BP W, Sfax 3038, Tunisia*
Tel. +216 96803179; email: omriabdesslem@yahoo.fr
[b]*Tunisian Chemical Group, B.P. 393/3018, Sfax, Tunisia*

Received 25 December 2012; Accepted 22 April 2013

ABSTRACT

Almond shell was used as a precursor to prepare activated carbon, using carbon dioxide as a physical activation agent. Its ability to remove the humic acid was evaluated. The surface area of almond shell activated carbon was found to be 1,310 m^2/g. The effects of experimental parameters such as pH, initial humic acid concentration, contact time, adsorbent dosage, and solution temperature on the adsorption were investigated. To describe the equilibrium isotherms the experimental data were analyzed by the Langmuir, Freundlich, and Temkin isotherm models. Pseudo-first-order, pseudo-second-order and intraparticle diffusion kinetic models were used to find out the kinetic parameters and mechanism of adsorption process. The thermodynamic parameters such as ΔG°, ΔH°, and ΔS° were calculated for predicting the nature of adsorption. For an approach to an industrial application, activated carbon prepared from almond shell seems to be an effective, low-cost, and good adsorbent precursor for the removal of humic acid from commercial phosphoric acid solution.

Keywords: Adsorption; Activated carbon; Humic acid; Isotherm; Kinetic

1. Introduction

Humic substances are the major organic constituents of river, lake, and pond waters. They are derived from soils, where they are formed through the breakdown of biomass by chemical and biological processes [1]. Humic acids are considered a problem for water supply industry. In fact, they adversely affect water quality in several ways. They not only cause undesirable color (yellowish to brownish) and taste [2], but also serve as food for bacterial growth in water distribution systems. Besides, together with heavy metals and biocides (pesticides and herbicides), humic acids yield high concentrations of these substances and enhance their transportation in water. Furthermore, their reaction with chlorine leads to the formation, but not to the evolution, of chlorinated organic

*Corresponding author.

Presented at the 6th International Conference on Water Resources in Mediterranean Basin (WATMED6), 10–12 October 2012, Sousse, Tunisia

compounds, some of which are known as human carcinogens (trihalomethanes). It was reported that an intake of a huge amount of humic acid might be one of the etiological factors for the blackfoot disease [3–5]. Thus, the removal of humic acids from the surface water or wastewater is very important.

Among the processes employed in water treatment, adsorption is considered an important method with high removal efficiency and no harmful by-products. Many kinds of adsorbents have been developed for the removal of humic acids from water, among which we can mention activated carbon [6–10], as well as resins [11], clays [12,13], zeolite [14–16], metal oxides [17], and biopolymers (chitosan) [18,19], as suggested in previous research studies. Although activated carbon exhibits a high surface area and high adsorption capacity, it has high operation costs and requires frequent regeneration. In recent years, the use of low-cost adsorbents has been of great interest. That is why several research studies have been conducted on wastes and residues for the adsorption of pollutant with varying success [20–24].

It is in this context that the present study lies, to report the use of almond shell activated carbon produced by pyrolysis and its physical activation in the presence of carbon dioxide, as an adsorbent to remove humic acids from aqueous solutions. Nowadays, this almond shell material, which is available in abundance in Sfax, Tunisia, is used principally as a solid fuel. The production of almond shell is estimated to exceed 60,000 t/year.

In the present investigation, almond shell-based activated carbon was prepared by physical activation for its potential to remove humic acid. The study includes an evaluation of the effects of various process parameters such as pH, contact time, initial concentration, and temperature. The experimental data are analyzed in terms of kinetic and equilibrium isotherm models. The results at different temperatures are used to evaluate thermodynamic parameters. Finally, an approach to the use of prepared activated carbon in an industrial application has been studied.

2. Materials and methods

2.1. Materials

Humic acid was obtained as a commercial, technical grade solid from Fluka. A 1 g/L concentration solution was prepared by dissolving 1 g of humic acid in 62.5 mL of NaOH solution (0.1 M) and completing at 1 L with deionized water. The solution was stirred for 1 h and stored.

2.2. Methods

2.2.1. Preparation of almond shell activated carbon

Almond shell used in this study was collected from a company "Chaabane" located in Sfax, Tunisia. After being cleaned with distilled water and dried at 110°C for 48 h, the sample was crushed with a blender and sieved to desired mesh size (1–2 mm). The carbonization of the raw shells and activation of the resulting chars were both carried out in a vertical stainless-steel reactor, which was placed in an electrical furnace Nabertherm. During the carbonization process, about 15 g of raw material was used to prepare the chars. The Nitrogen gas at a flow rate of 150 cm^3/min, was passed through the reactor, right from the beginning of the carbonization process. Next, the furnace temperature was increased at a rate of 5°C/min from room temperature to 450°C and held at this temperature for 1 h. The activation was carried out in the same furnace. The charcoal obtained was then physically activated at 850°C for 2 h under a CO_2 flow (100 cm^3/min). After activation, the sample was cooled to ambient temperature under N_2 flow rate. The produced activated carbon was then dried at 105°C overnight, ground and sifted to obtain a powder with a particle size smaller than 45 μm, and finally kept in hermetic bottle for subsequent use.

2.2.2. Characterization of almond shell activated carbon

The surface area was determined by nitrogen adsorption at −196°C with an automatic adsorption instrument (ASAP 2010, Micromeritics). Prior to the measurements, the samples were out-gassed at 300°C under nitrogen for at least 24 h. The amount of N_2 adsorbed at relative pressures near unity (≈0.99) corresponds to the mole number of adsorbed nitrogen per gram of activated carbon. With regard to the surface area of the sample, it was calculated by Brunauer–Emmet–Teller method in relative pressure (P/P_0) range of 0.05–0.30 at −196°C. As for the surface functional group of the prepared activated carbon, it was detected by Fourier Transform Infrared (FTIR) spectroscope (NICOET spectrometer) whose spectra were recorded from 4,000 to 500 cm^{-1}. Concerning the surface morphology of the activated sample, it was examined using a scanning electron microscope (Philips XL30 microscope).

The well-known Boehm's method allows the modeling of the principal acidic oxygenated functions of the activated carbon such as carboxylic acids, lactones, and phenols using bases of increasing strength as $NaHCO_3$, Na_2CO_3, and NaOH, respectively. Then, the

total basicity is given by titration of HCl. More details are given in Refs. [25,26].

The point of zero charge (pH_{PZC}) characteristic of the almond shell activated carbon was determined using the solid addition method [27].

2.2.3. Adsorption experiments

The effects of experimental parameters such as, initial humic acid concentration (10–100 mg/L), pH (3–10), adsorbent dosage (0.01–0.09 g), and temperature (298–318 K) on the adsorptive removal of humic acids were studied in a batch mode of operation for a specific period of contact time (60–600 min) at a fixed speed of 200 rpm. While pH was adjusted using 0.1 N HCl or 0.1 N NaOH, batch equilibrium adsorption experiments were performed using 100 mL of humic acid. After adsorption process the adsorbent was separated from the samples by filtering through filter paper (pore size: 0.45 μm) and the filtrate was analyzed using UV–vis spectrophotometer (UV-1650PC Shimadzu, Japan) at its maximum wavelength of 254 nm. The amount of adsorption at equilibrium q_e (mg/g) was calculated by the following equation:

$$q_e = \frac{(C_0 - C_e) \times V}{m} \quad (1)$$

where C_0 and C_e (mg/L) are the liquid-phase concentrations of humic acid initially and at equilibrium, respectively. V is the volume of the solution (L) and m is the mass of dry adsorbent used (g). Adsorption isotherms were obtained by plotting adsorption capacities with respect to the equilibrium concentrations.

2.2.4. Equilibrium modeling

Adsorption is a well-known equilibrium separation process for wastewater treatment. Its isotherms are the equilibrium relationships between the concentrations of the adsorbed humic acid and humic acid in the solution at a given temperature. In this study, Langmuir, Freundlich, and Temkin isotherm models were used to investigate the adsorption equilibrium between the humic acid in the solution and the activated carbon phase.

The Langmuir model is a non-linear model that suggests a monolayer uptake of the humic acid on a homogenous surface, having uniform energies of adsorption for all the binding sites without any interaction between the adsorbent molecules [28]. The linear form of the Langmuir isotherm equation [29,30] is represented by the following equation:

$$\frac{C_e}{q_e} = \frac{1}{Q_m b} + \frac{C_e}{Q_m} \quad (2)$$

where C_e is the equilibrium concentration of the adsorbate (mg/L), q_e is the amount of adsorbate adsorbed per unit mass of adsorbent (mg/g), b the Langmuir adsorption constant (L/mg), and Q_m is the theoretical maximum adsorption capacity (mg/g).

The Langmuir parameters can be used to predict the affinity between the adsorbate and adsorbent using dimensionless separation factor (R_L). R_L is calculated by the following equation [31]:

$$R_L = \frac{1}{1 + bC_0} \quad (3)$$

The value of R_L indicates the shape of the isotherm to be either unfavorable ($R_L > 1$), linear ($R_L = 1$), favorable ($0 < R_L < 1$), or irreversible ($R_L = 0$).

The Freundlich isotherm is an empirical model that is based on adsorption on heterogeneous surface and active sites with different energies. The linearized Freundlich isotherm equation [32] is represented by the following equation:

$$\log q_e = \log K_F + \left(\frac{1}{n} \log C_e\right) \quad (4)$$

where K_F and n are Freundlich constants with n as a measure of the deviation of the model from linearity of the adsorption and K_F (mg/g(L/mg)$^{1/n}$) indicates the adsorption capacity of the adsorbent. In general, $n > 1$ suggests that adsorbate is favorably adsorbed on the adsorbent. The higher the 1/n value, the stronger the adsorption intensity.

Temkin and Pyzhev [33,34] considered the effects of indirect adsorbent/adsorbate interactions on adsorption isotherms. The heat of the adsorption of all the molecules in the layer would decrease linearly with coverage due to adsorbent/adsorbate interactions. The linear form of Temkin isotherm equation is as follows:

$$q_e = \left(\frac{RT}{b_T}\right) \ln A + \left(\frac{RT}{b_T}\right) \ln C_e \quad (5)$$

where $B = RT/b_T$, b_T is the Temkin constant relates to the heat of sorption (J/mol), A is the Temkin isotherm constant (L/g), R the gas constant (8.314 J/mol K), and T the absolute temperature (K).

2.2.5. Kinetic modeling

The kinetics of adsorption is an important characteristic to define the efficiency of adsorption. In order to investigate the mechanism of adsorption and kinetic parameters, sorption data was analyzed using pseudo-first-order [35,36], pseudo-second-order [37,38], and intraparticle diffusion [39] models.

The pseudo-first-order kinetic model found by Lagergren is widely used to predict sorption kinetic and is defined as:

$$\log(q_e - q_t) = \log q_e - \frac{k_1}{2.303}t \quad (6)$$

where q_e and q_t are the amounts adsorbed at equilibrium and at time t (mg/g), and k_1 is the rate constant of the pseudo-first-order adsorption (min^{-1}).

The pseudo-second-order kinetic model equation is expressed as:

$$\frac{t}{q_t} = \frac{1}{k_2 q_e^2} + \frac{1}{q_e}t \quad (7)$$

where k_2 (g/mg min) is the rate constant of second-order adsorption. The linear plot of t/q_t vs. t gives $1/q_e$ as the slope and $1/k_2{q_e}^2$ as the intercept.

The kinetic results were further analyzed for the diffusion mechanism, by means of the intraparticle diffusion model. The intraparticle diffusion equation is expressed as:

$$q_t = k_{int}t^{\frac{1}{2}} + C \quad (8)$$

where k_{int} is the intraparticle diffusion rate constant (mg/g $min^{1/2}$) and C is the intercept, which represents the thickness of the boundary layer. If intraparticle diffusion occurs, then q_t vs. $t^{1/2}$ will be linear and if the plot passes through the origin, then the rate limiting step is only due to the intraparticle diffusion. Otherwise, some other mechanisms along with intraparticle diffusion are involved. In most cases, this plot gives general features of three stages; the first of which is an initial curved portion, the second is an intermediate linear portion, and the third is a plateau. Regarding the initial sharper, it is due to the instantaneous adsorption or external surfacing adsorption (external mass transfer). With respect to the intermediate linear part, it is due to intraparticle diffusion. As for the plateau, it is due to the equilibrium stage, in which the intraparticle diffusion starts to slow down owing to the extremely low solute concentrations in the solution [40].

2.2.6. Thermodynamic modeling

The temperature dependence of the adsorption process is associated with several thermodynamic parameters. Besides, the thermodynamic considerations of an adsorption process are necessary to conclude whether the process is spontaneous or not. There are three thermodynamic parameters that must be considered to characterize the adsorption process, which are the standard enthalpy (ΔH°, kJ/mol), standard free energy (ΔG°, kJ/mol), and standard entropy (ΔS°, kJ/mol K). The values of ΔH°, ΔG°, and ΔS° can be obtained from the following Eqs. (9) and (10) [41]:

$$\Delta G = -RT\mathrm{Ln}K \quad (9)$$

$$\Delta G = -\Delta H - T\Delta S \quad (10)$$

where R is the universal gas constant (8.314 J/mol K), T is the temperature (K), and K is the Langmuir isotherm constant. While the Langmuir constant (l/mol) can be obtained from the plot of C_e/q_e vs. C_e, the ΔH° and ΔS° values can be calculated from the slope, intercept of a plot of ΔG° vs. T.

3. Results and discussion

3.1. Physical and chemical characterization of adsorbent

Surface area is one of the most important properties of adsorbents. Fig. 1 shows nitrogen adsorption/desorption isotherm curve onto the activated carbon prepared at −196°C. In fact, the obtained isotherm curve belongs to a mixed type in the IUPAC classification, type I at low pressure and type IV at intermediate and high P/P_0. In the initial part, they are type I, with an important uptake at relatively low pressures,

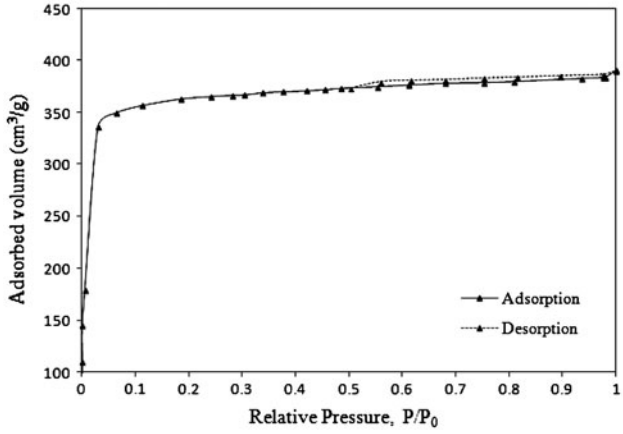

Fig. 1. Nitrogen adsorption–desorption isotherms of almond shell activated carbon.

which is the characteristic of microporous materials. However, in the curve presented, there is no clear plateau but certain slopes can be observed at intermediate and high relative pressures. All these facts indicate the transition from microporosity to mesoporosity (type IV). Moreover, a desorption hysteresis loop due to adsorbate condensation in the mesopores is presented. The adsorption isotherm of this material has shown good agreement with those reports in the literature [42,43].

The microstructure of the raw material and resulting activated carbon in Fig. 2 shows that the adsorbent gives a rough texture with a heterogeneous surface and a variety of randomly distributed pore size. Furthermore, it contains an irregular and highly porous surface, indicating a relatively high surface area. This observation can be supported by the high value of the BET surface area of the prepared activated carbon as illustrated in Table 1.

Table 1
Porous structure parameters of the activated carbon

Parameters	Values
BET surface area, S_{BET} (m^2/g)	1,310.134
Pore volume (cm^3/g)	0.621
Average pore diameter (Å)	1.896

Table 2
Concentrations (meq/g) of acidic and basic groups of the surface in activated carbon

Surface functions	Values
Total of acid functions	2.606
Carboxylic (–COOH)	1.604
Lactones (–COO–)	0.875
Phenol (–OH)	0.127
Total of basic functions	1.598

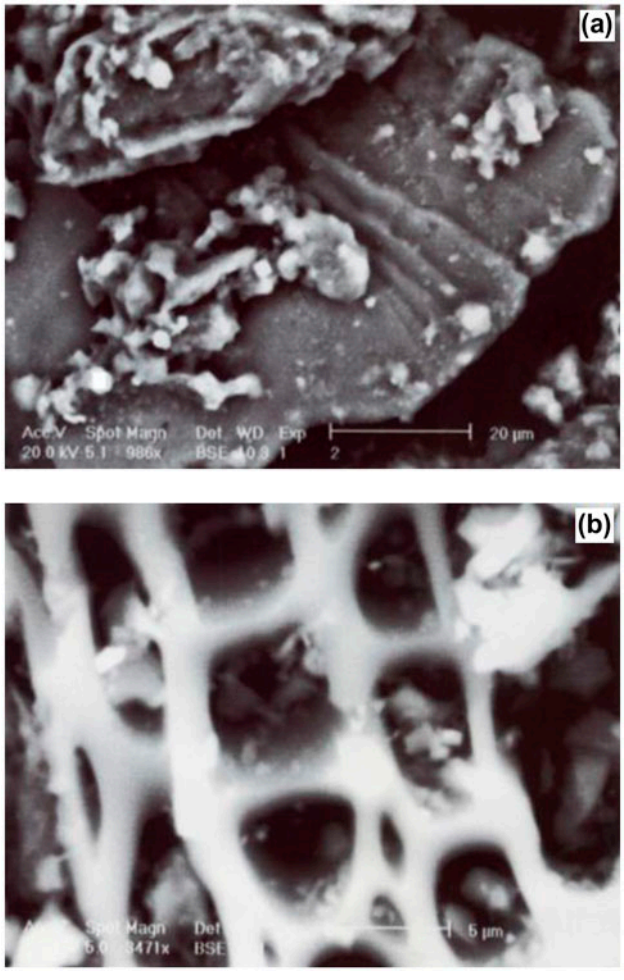

Fig. 2. SEM micrographs of almond shell (a) and prepared activated carbon (b).

The analysis of surface functions covering the carbons made it possible to identify the acid and base groupings. Some examples of oxygen containing functionalities detected on the carbon surface include the following: carboxylic, lactone, phenol, carbonyl, pyrone, chromene, quinone, and ether groups [44]. The results of the analysis of the surface oxygen functional groups of our activated carbon product presented in Table 2, lead to the conclusion that the quantity of the acidic functions is much more important than those of the basic functions. So we can conclude that the activated carbons are of the type acids.

Additionally, as presented in Fig. 3, the information about the chemical structure and functional groups is determined by the infrared spectroscopy of the prepared adsorbent. The band located at 3,447 cm^{-1} is attributed to ν(O–H) vibrations in hydroxyl groups. Besides, the weak and broad peaks that appear at 2,254 cm^{-1} could be assigned to ν (C≡C) vibrations in alkyne groups. Next, while the skeletal C=C vibrations in aromatic rings cause the absorptions in 1,585 cm^{-1}, the absorptions at 1,438 cm^{-1} could be the result of C–O stretching in carboxylate groups. Concerning the peaks at 1,130 cm^{-1}, they are due to the vibrations of C–O stretching. As for the C–H out-of-plane bending in benzene derivative vibrations, it causes the band at 890 cm^{-1} [45].

3.2. Effect of contact time and humic acid initial concentration

In order to determine the equilibrium time for maximum uptake, a contact time study was

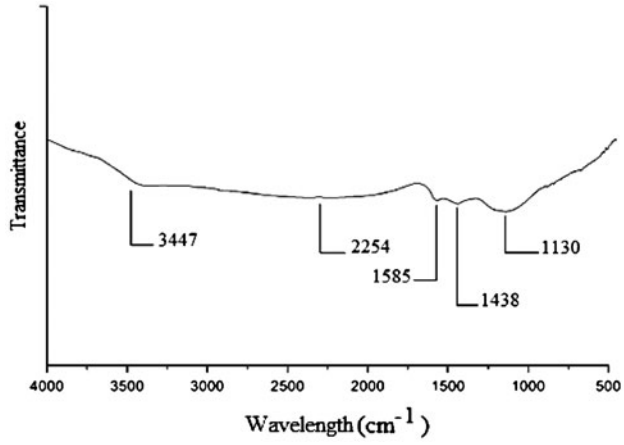

Fig. 3. FT-IR spectra of almond shell activated carbon.

performed with different initial concentrations of humic acid of 10, 40, 70, and 100 mg/L. A graphical representation of the contact time as a function of initial concentrations, as given in Fig. 4 suggests that the adsorption increased sharply with contact time in the first 180 min and equilibrium adsorption was established within 300 min. As shown in Fig. 4, the rate of adsorption of the acid was initially rapid and then it gradually slowed until it reached equilibrium; once equilibrium was reached (300 min), there was no significant increase in the humic acid removal. This observation can be explained by the fact that the adsorption rate is fast at the beginning, because the acid is adsorbed by the exterior surface of the activated carbon. When the exterior adsorption surface reaches saturation, the humic acid enters into the pores of the adsorbent and is adsorbed by the interior surface of the particles. This phenomenon requires a relatively long contact time.

3.3. Effect of solution temperature

Adsorption experiments were conducted at 298, 308, and 318 K to investigate the effect of temperature, with initial humic acid concentration of 10–100 mg/L (Fig. 5). It was observed that the maximum adsorption of humic acid increased from 136.25 mg/g at 298 K to 152.72 mg/g at 318 K for initial concentration equal to 100 mg/L, i.e. adsorption increased with the increase in temperature, indicating better adsorption at higher temperatures, i.e. endothermic process. The increase in the amount of humic acid adsorbed at equilibrium with an increase in temperature may either be attributed to the acceleration of some originally slow adsorption steps or to the creation of some new active sites on the adsorbent surface. The enhanced mobility of humic acid from the bulk solution towards the adsorbent surface should be taken into account. It is worthwhile to note in this case that the adsorption interaction involves some types of specific interaction at higher temperature, which indicates that the adsorption process is endothermic. Alternatively, such behavior may be ascribed to the "activated" adsorption which accelerates the diffusion into certain pores in the adsorbent [46]. These results are similar to other studies [47,48].

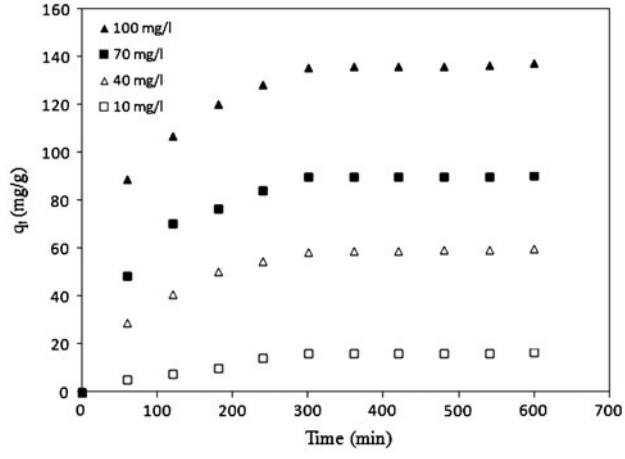

Fig. 4. Effect of contact time on the adsorption of humic acid by almond shell activated carbon at various concentrations (adsorbent dosage = 0.05 g; pH = 3; temperature = 298 K).

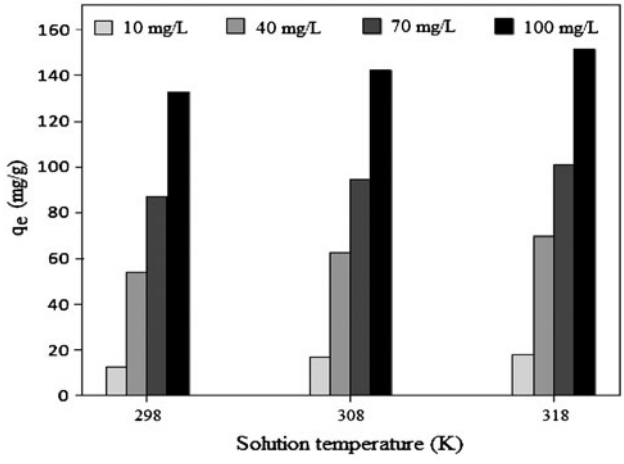

Fig. 5. Effect of solution temperature on humic acid adsorption at various initial concentrations. (contact time = 300 min; pH = 3; adsorbent dosage = 0.05 g).

3.4. Effect of pH

The effect of pH on the adsorption of humic acid on prepared activated carbon was studied by varying the initial pH values of the humic acid solutions from 2 to 9, as shown in Fig. 6. Indeed, the pH value of the solution is an important controlling parameter in the adsorption process. The removal of humic acid from aqueous solution by the activated carbon decreases significantly with the increase in pH. It was observed that the maximum adsorption of humic acid was achieved at pH = 3. At the initial humic acid solution concentration of 40 mg/L, an increase in the pH from 2 to 9 substantially decreased the adsorption amount from 57.82 to 15.32 mg/g. It has been reported that humic acid adsorption onto other adsorbents, such as activated carbon prepared from biomass material, acid-activated Greek bentonite, and montmorillonite-Cu(II)/Fe(III) oxide magnetic material also follow similar trends [19,49,50]. In general, the humic acid consists of many polymeric components with major functional groups as carboxylic and phenolic, which can be ionized by increasing water pH to exhibit anionic characteristics. At high pH, the anionic species from humic acid will compete with OH^- to occupy the active solid sites, thus resulting in the decrease of humic acid adsorption. At low pH, high adsorption of this acid can be attributed to the charge reduction of the weakly acidic humic acids as the pH was lowered [10]. In addition, the pH_{PZC} value of almond shell activated carbon was 3.59. Thus, the activated carbon presents positive charge at pH < 3.59, but negative charge at pH > 3.59. Due to the increasing electrostatic repulsion between surface negative charge on the solids and humic acid, the adsorption will progressively decrease with the increase in pH.

3.5. Effect of adsorbent dosage

The effect of adsorbent dosage on the adsorption of humic acid by almond shell activated carbon is presented in Fig. 7. The amount of adsorption increased from 12.04 to 57.61 mg/g as the activated carbon dose increased from 0.01 to 0.05 g and then remained almost constant. The increased adsorption at high dosages is expected owing to the increased adsorbent surface area and availability of more adsorption sites [51]. The optimum dosage was found to be 0.05 g.

3.6. Adsorption isotherms

The Langmuir, Freundlich, and Temkin isotherm parameters for adsorption of humic acid onto activated carbon are given in Table 3. The comparison of the R^2 values shows that the Langmuir isotherm goes quite well with the experimental data having a high correlation coefficient. This result may be due to the homogenous distribution of active sites on the surface of adsorbent. The calculated R_L value was greater than zero and less than unity, showing favorable adsorption of humic acid onto activated carbon obtained from almond shell by physical activation with CO_2. The values of n were found to be less than 10 indicating that the adsorption was favorable. As can be further seen from Table 3, the values of

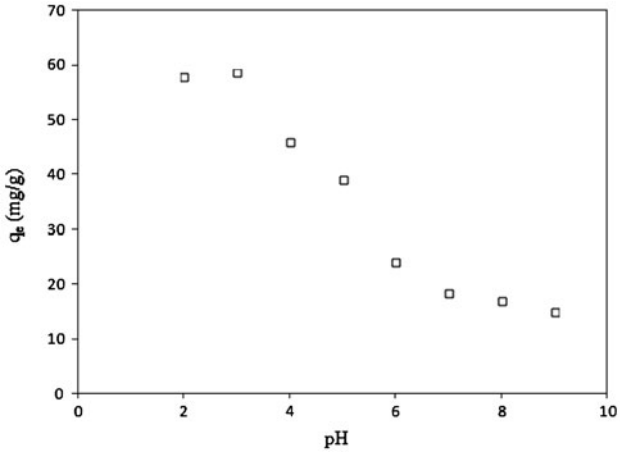

Fig. 6. Effect of pH on the adsorption of humic acid by prepared activated carbon (initial humic acid concentration C_0 = 40 mg/L; temperature = 298 K; contact time = 300 min; adsorbent dosage = 0.05 g).

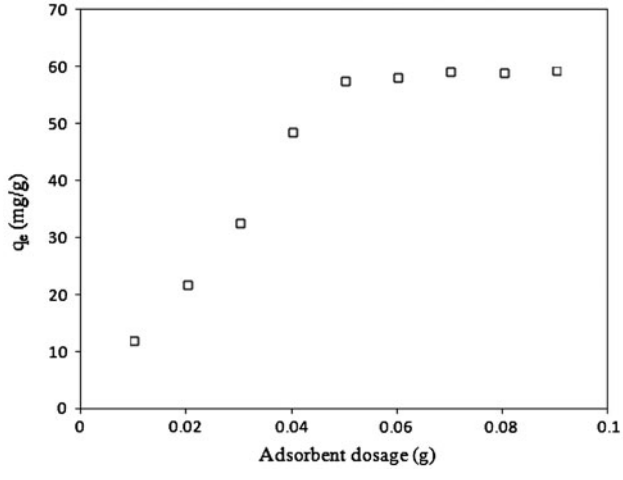

Fig. 7. Effect of adsorbent dosage on the adsorption of humic acid by prepared activated carbon (initial humic acid concentration C_0 = 40 mg/L; temperature = 298 K; contact time = 300 min; pH = 3).

Table 3
Isotherm constants for humic acid adsorption onto almond shell activated carbon at different temperatures

Isotherm	Temperatures		
	298 K	308 K	318 K
Langmuir isotherm			
Q_m (mg/g)	120.481	151.515	169.592
b (l/mg)	0.046	0.08	0.256
R_L	0.236	0.151	0.055
R^2	0.981	0.991	0.992
Freundlich isotherm			
K_F (mg/g) (l/mg)$^{1/n}$	9.479	13.661	37.462
n	1.370	1.494	2.854
R^2	0.986	0.977	0.980
Temkin isotherm			
b_T (J/mol)	77.0	82.021	115.77
A (L/g)	0.617	0.918	4.237
R^2	0.985	0.982	0.988

Table 4
Comparison of adsorption capacity of humic acid with other reported adsorbents

Adsorbent	C_0 (mg/L)	T (K)	Q_m (mg/g)	Reference
Activated carbon (rice husk)	20–150	308	54.4	[9]
Acid-activated Greek bentonite	10–200	318	10.81	[48]
Fly ash	50	303	10.7	[49]
Unburned carbon	50	303	71.8	[49]
Aminated polyacrylonitrile fibers	10–100	296	16.22	[52]
Chitosan–ECH beads	10–50	300	44.84	[53]
Almond shell activated carbon	10–70	318	169.592	This study

Q_m and K_F increased with temperature, indicating that the adsorption process was endothermic by nature.

It is also important to compare the value of maximum adsorption capacity obtained from this study with the values from other reported adsorbents, since this will suggest the effectiveness of almond shell activated carbon as a potential adsorbent for the treatment of water containing humic acid. The adsorption capacity for humic acid using this prepared activated carbon is comparable with other reported adsorbents as shown in Table 4.

3.7. Thermodynamic parameters

The calculated values of ΔH°, ΔS°, and ΔG° for adsorption of humic acid on prepared activated carbon are shown in Table 5. The positive ΔH° value indicated that the adsorption process was endothermic in nature which is consistent with the results obtained earlier when the humic acid uptake increases with increasing solution temperature. The positive values of ΔS° showed the affinity of the adsorbent for adsorbate and the increasing randomness at the solid–solution interface with some structural changes in the

Table 5
Thermodynamic parameters for adsorption of humic acid on almond shell activated carbon

ΔH (kJ/mol)	ΔS (kJ/molK)	ΔG (kJ/mol)		
		298 K	308 K	318 K
81.238	0.286	−4.242	−6.388	−9.969

Table 6
Kinetic model parameters for adsorption of humic acid onto prepared activated carbon

Kinetic model	C_0 (mg/L)			
	10	40	70	100
q_e,exp (mg/g)	16.21	58.603	90.01	136.09
Pseudo-first-order				
q_e, cal (mg/g)	30.91	104.93	57.279	66.834
k_1 (min^{-1})	0.012	0.014	0.014	0.008
R^2	0.954	0.907	0.925	0.890
Pseudo-second-order				
q_e, cal (mg/g)	20.964	67.567	99.009	147.058
k_2 (g mg^{-1}min)	0.014	0.0002	0.0004	0.00001
R^2	0.980	0.995	0.996	0.998
Intraparticle diffusion model				

adsorbates and adsorbents during the adsorption process. The free energy changes (ΔG°) were negative, reflecting the spontaneity and feasibility of these processes.

3.8. Kinetic study

Pseudo-first-order, pseudo-second-order, and intraparticle diffusion kinetic parameters are represented in Table 6. The correlation coefficient for the pseudo-second-order kinetic model was higher than the one for pseudo-first-order kinetic model. This indicates that the adsorption perfectly complies with pseudo-second-order reaction and the adsorption of humic acid process appeared to be controlled by the chemisorptions process. The adsorption mechanism can be described by the intraparticle diffusion by plotting the quantity of humic acid adsorbed against square root of time as shown in Fig. 8. It can be observed that the plots are not linear over the whole time range and the graphs of this figure reflect a dual nature, with initial linear portion followed by a plateau. The fact that the first curved portion of the plots seems to be absent, implies that the external surface adsorption (stage 1) is relatively very fast and the stage of intra-particle diffusion (stage 2) is attained 300 min. Finally, equilibrium adsorption (stage 3) starts after 300 min. The humic acid molecules are slowly transported via intraparticle diffusion into the particles and finally retained in the pores.

The results obtained are in harmony with those found by Monser and Adhoum [54] for the adsorption of tartrazine onto activated carbon.

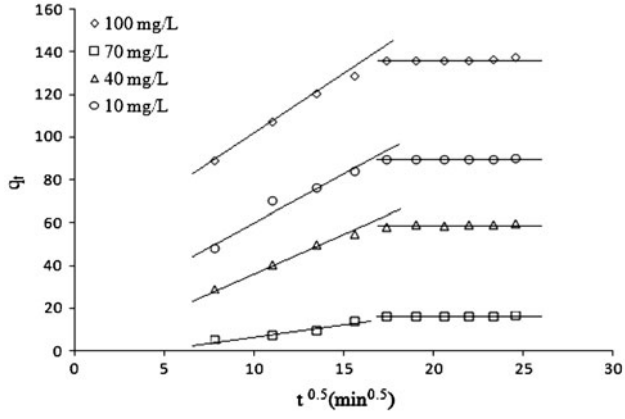

Fig. 8. Intraparticle diffusion plots for adsorption of humic acid onto prepared activated carbon (temperature = 298 K; adsorbent dose = 0.05 g, min, pH = 3).

4. Approach to industrial application

The prepared activated carbon has very developed textural and structural properties (specific surface >1,310 m^2/g) thanks to the presence of different functional groups (hydroxyl and carboxyl function) to the prepared surface. Therefore this adsorbent can be used for industrial application. The humic acid is presented initially in the industrial phosphoric acid which is manufactured from phosphate rock by the SIAPE society using wet process [55,56]. The ultimate objective of the present study is to achieve an experimental approach by determining the percentage removal of humic acid added to a commercial solution of phosphoric acid.

4.1. Adsorption experiments of humic acid from commercial phosphoric acid

All the experiments were carried out in the following manner: A 0.5 g amount of the prepared activated carbon was placed in Erlenmeyer flasks of 250 mL capacity in contact with 100 mL of commercial industrial phosphoric acid solution (1 mol/L) initially mixed with 5 mg of humic acid at a temperature of 50°C under constant agitation (400 rpm) and a pH value to 1. A reflux refrigerant was placed on each Erlenmeyer to avoid water evaporation. After the desired contact time, the carbon particles and the supernatant acid were separated by filtration on an organic membrane of convenient porosity. The filtrate was measured using UV–vis spectrophotometer.

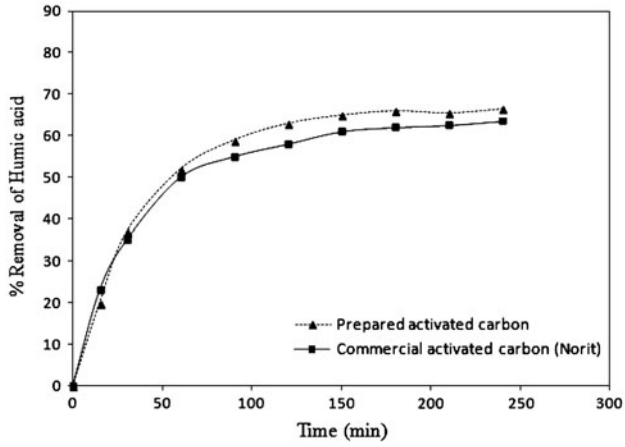

Fig. 9. A comparison of activated carbon and commercial activated carbon (temperature = 50 °C; agitation speed = 400 rpm).

The removal efficiency of humic acid by prepared activated carbon was calculated as follows:

$$\% \text{ removal} = \frac{C_0 - C_r}{C_0} \times 100 \quad (11)$$

Where C_0 and C_r are the initial and residual concentrations of humic acid from commercial phosphoric acid, respectively (mg/L).

4.2. Comparison with commercially available adsorbent material

Fig. 9 provides a comparison of removal capability of the prepared activated carbon and the commercial activated carbon (Norit, $S_{BET} = 491\ m^2/g$) designed for humic acid removal. This figure shows that the tested commercial carbon has lower performance compared to the prepared activated carbon. The removal of humic acid onto two types of the activated carbon increases with time and then attains equilibrium value at a time of about 180 min. The maximum percentage removal of humic acid reaches 68% at 50 °C. The percentage removal of humic acid by activated carbon prepared is related to its physico-chemical properties.

5. Conclusions

In the present study, the adsorption of humic acid is found to increase with the increase in contact time, acid initial concentration, adsorbent dose and solution temperature. The solution pH <3 was proved to be more favorable for adsorption of humic acid on the almond shell activated carbon. The Langmuir isotherm model and the pseudo-second-order kinetic model were found to be in accordance with the adsorption data well. The intraparticle diffusion model could well explain the adsorption process which was found to be controlled by external mass transfer at earlier stages and by intraparticle. From the thermodynamic studies, the adsorption process was endothermic and spontaneous by nature. Almond shell activated carbon is shown to be a promising adsorbent for the removal of humic acid from aqueous solution over a wide range of concentrations. Concerning the approach to an industrial application, the activated carbon prepared from almond shell can be used for the removal of humic acid from industrial phosphoric acid solution.

Acknowledgments

The authors gratefully acknowledge financial support from the Tunisian Chemical Group. They also wish to express their gratitude to Mr. A. Charfi, Mr. L. Fourati, K. Foued, and Mme F. Bennour Mrad for their help and support. Thanks are due to Mr. Z. Fakhfakh from Faculty of Science of Sfax for the assistance in MEB. Also, I thank Mme. L. Mahfoudhi for this linguistic assistance in this manuscript.

Nomenclature

BET	—	Brunauer–Emmet–Teller
pH_{PZC}	—	pH of the point of zero charge
q_e	—	amount of humic acid adsorbed at equilibrium (mg/g)
q_t	—	amount of humic acid adsorbed at any time t (mg/g)
t	—	time (min)
C_0	—	initial concentration of the humic acid (mg/L)
C_e	—	concentrations of humic acid at equilibrium (mg/L)
C_r	—	residual concentration
V	—	solution volume (L)
m	—	mass of dry adsorbent (g)
Q_m	—	Langmuir constant; theoretical maximum adsorption capacity (mg/g)
b	—	Langmuir adsorption constant (L/mg)
R_L	—	dimensionless separation factor
K_F	—	Freundlich constant indicative of the relative adsorption capacity of the adsorbent $(mg/g(L/mg)^{1/n})$
n	—	Freundlich constant indicative of the intensity of the adsorption
R	—	universal gas constant (J/molK)

T	—	temperature (K)
b_T	—	Temkin constant relates to the heat of adorption (J/mol)
k_1	—	pseudo-first-order rate constant (min^{-1})
k_2	—	pseudo-second-order rate constant (g/mg min)
k_{int}	—	intraparticle diffusion rate constant ($mg/g\,min^{1/2}$)
C	—	thickness of the boundary layer
ΔG°	—	standard free energy (kJ/mol)
ΔH°	—	standard enthalpy (kJ/mol)
ΔS°	—	standard entropy (kJ/molK)

References

[1] S. Boggs, D. Livermore, M.G. Seitz, Humic substances in natural waters and their complexation with trace metals and radionuclides: A review report, Macromol. Chem. Phys. 25 (1985) 599–657.

[2] O.D. Basu, P.M. Huck, Integrated biofilter-immersed membrane system for the treatment of humic waters, Water Res. 38(3) (2004) 655–662.

[3] E. Lorenc-Grabowska, G. Gryglewicz, Adsorption of lignite-derived humic acids on coalbased mesoporous activated carbons, J. Colloid Interface Sci. 284 (2005) 416–423.

[4] M. Nystrom, K. Ruohomaki, L. Kaipia, Humic acid as a fouling agent in filtration, Desalination 106 (1996) 79–87.

[5] X. Peng, Z. Luan, F. Ch, B. Tian, Z. Jia, Adsorption of humic acid onto pillared bentonite, Desalination 174 (2005) 135–143.

[6] J.P. Chen, S. Wu, Simultaneous adsorption of copper ions and humic acid onto an activated carbon, J. Colloid Interface Sci. 280 (2004) 334–342.

[7] S. Maghsoodloo, B. Noroozi, A.K. Haghi, G.A. Sorial, Consequence of chitosan treating on the adsorption of humic acid by granular activated carbon, J. Hazard. Mater. 191 (2011) 380–387.

[8] M.S. Rauthula, V.C. Srivastava, Studies on adsorption/desorption of nitrobenzene and humic acid onto/from activated carbon, Chem. Eng. J. 168 (2011) 35–43.

[9] A.A.M. Daifullah, B.S. Girgis, H.M.H. Gad, A study of the factors affecting the removal of humic acid by activated carbon prepared from biomass material, Colloids Surf. A 235 (2004) 1–10.

[10] S. Han, S. Kim, H. Lim, W. Choi, H. Park, J. Yoon, T. Hyeon, New nanoporous carbon materials with high adsorption capacity and rapid adsorption kinetics for removing humic acids, Microporous Mesoporous Mater. 58 (2003) 131–135.

[11] J. Wang, Y. Zhou, A. Li, L. Xu, Adsorption of humic acid by bi-functional resin JN-10 and the effect of alkali-earth metal ions on the adsorption, J. Hazard. Mater. 176 (2010) 1018–1026.

[12] M. Salmana, B. El-Eswed, F. Khalili, Adsorption of humic acid on bentonite, Appl. Clay Sci. 38 (2007) 51–56.

[13] J.Q. Jiang, C. Cooper, Preparation of modified clay adsorbents for the removal of humic acid, Environ. Eng. Sci. 20 (2003) 581–586.

[14] S. Wang, T. Terdkiatburana, M.O. Tadé, Adsorption of Cu(II), Pb(II) and humic acid on natural zeolite tuff in single and binary systems, Sep. Purif. Technol. 62 (2008) 64–70.

[15] S.G. Wang, W.X. Gong, X.W. Liu, B.Y. Gao, Q.Y. Yue, Removal of fulvic acids using the surfactant modified zeolite in a fixed-bed reactor, Sep. Purif. Technol. 51 (2006) 367–373.

[16] S. Capasso, S. Salvestrini, E. Coppola, A. Buondonno, C. Colella, Sorption of humic acid on zeolitic tuff: A preliminary investigation, Appl. Clay Sci. 28 (2005) 159–165.

[17] E.K. Kim, H.W. Walker, Effect of cationic polymer additives on the adsorption of humic acid onto iron oxide particles, Colloids Surf. A 194 (2001) 123–131.

[18] M. Chang, R. Juang, Adsorption of tannic acid, humic acid, and dyes from water using the composite of chitosan and activated clay, J. Colloid Interface Sci. 278 (2004) 18–25.

[19] X. Zhang, R. Bai, Mechanisms and kinetics of humic acid adsorption to chitosan-coated granules, J. Colloid Interface Sci. 264 (2004) 30–38.

[20] M. Belhachemi, F. Addoun, Adsorption of congo red onto activated carbons having different surface properties: Studies of kinetics and adsorption equilibrium, Desalin. Water Treat. 37 (2012) 122–129.

[21] G. Issabayeva, M.K. Aroua, N.M. Sulaiman, Study on palm shell activated carbon adsorption capacity to remove copper ions from aqueous solutions, Desalination 262 (2010) 94–98.

[22] A. Omri, M. Benzina, Adsorption characteristics of silver ions onto activated carbon prepared from almond shell, Desalin. Water Treat. iFirst (2012) 1–10. doi: 10.1080/19443994.2012.734585.

[23] A. Omri, A. Wali, M. Benzina, Adsorption of bentazon on activated carbon prepared from Lawsonia inermis wood: Equilibrium, kinetic and thermodynamic studies, Arab. J. Chem. (2012), doi: 10.1016/j.arabjc.2012.04.047.

[24] A. Omri, M. Benzina, Removal of manganese(II) ions from aqueous solutions by adsorption on activated carbon derived a new precursor: Ziziphus spina-christi seeds, Alexandria Eng. J. 51 (2012) 343–350.

[25] J. Starck, P. Burg, D. Cagniant, J.M.D Tascon, A. Martinez-Alonso, The effect of demineralisation on a lignite surface properties, Fuel 83 (2004) 845–850.

[26] H.P. Boehm, Some aspects of the surface chemistry of carbon blacks and other carbons, Carbon 32 (1994) 759–769.

[27] A. Kumar, B. Prasad, I.M. Mishra, Adsorptive removal of acrylonitrile by commercial grade activated carbon: Kinetics, equilibrium and thermodynamics, J. Hazard. Mater. 152 (2008) 589–600.

[28] M.F. Sawalha, J.R. Peralta-Videa, J. Romero-Gonzales, J.L. Gardea-Torresdey, Biosorption of Cd(II), Cr(III), and Cr(IV) by saltbush (Atriplexcanescens) biomass: Thermodynamic and isotherm studies, J. Colloid Interface Sci. 300 (2006) 100–104.

[29] I. Langmuir, The constitution and fundamental properties of solids and liquids, J. Am. Chem. Soc. 38 (1916) 2221–2295.

[30] I. Langmuir, The adsorption of gases on plane surfaces of glass, mica and platinum, J. Am. Chem. Soc. 40 (1918) 1361–1403.

[31] T.W. Weber, R.K. Chakravorti, Pore and solid diffusion models for fixed bed adsorbents, J. Am. Inst. Chem. Eng. 20 (1974) 228–238.

[32] H.M.F. Freundlich, Uber die adsorption in lösungen [Ber die adsorption in lo sungen], Z. Phys. Chem. 57 (1906) 385–470.

[33] M.J. Temkin, V. Phyzev, Recent modifications to Langmuir isotherms, Acta Physiochim, USSR 12 (1940) 217–222.

[34] M.J. Temkin, V. Phyzev, Kinetic of ammonia synthesis on promoted iron catalysts, Acta Physiochim, USSR 12 (1940) 237–356.

[35] S. Lagergren, Zur theorie der sogenannten adsorption gelöster stoffe, Kungliga Svenska Vetenskapsakademiens. Handlingar 24 (1898) 1–39.

[36] J. Febrianto, A.N. Kosasih, J. Sunarso, Y.H. Ju, N. Indraswati, S. Ismadji, Equilibrium and kinetic studies in adsorption of heavy metals using biosorbent: A summary of recent studies, J. Hazard. Mater. 162 (2009) 616–645.

[37] Y.S. Ho, G. McKay, Pseudo-second order model for sorption process, Process Biochem. 34 (1999) 451–465.

[38] Y.S. Ho, G. McKay, D.A.J. Wase, C.F. Foster, Study of the sorption of divalent metal ions on the peat, Adsorp. Sci. Technol. 18 (2000) 639–650.

[39] W.J. Weber, J.C. Morriss, Kinetics of adsorption on carbon from solution, J. Sanit. Eng. Div. Am. Soc. Civil Eng. 89 (1963) 31–60.

[40] A.A.M. Daifullah, S.M. Yakout, S.A. Elreefy, Adsorption of fluoride in aqueous solutions using KMnO4-modified activated carbon derived from steam pyrolysis of rice straw, J. Hazard. Mater. 147 (2007) 633–643.
[41] L. Wang, J. Zhang, R. Zhao, C. Li, Y. Li, C.L. Zhang, Adsorption of basic dyes on activated carbon prepared from polygonum orientale linn: Equilibrium, kinetic and thermodynamic studies, Desalination 254 (2010) 68–74.
[42] A.M. Puziy, O.I. Poddubnaya, A. Martinez-Alonso, F. Suarez-Garcia, J.M.D. Tascon, Synthetic carbons activated with phosphoric acid: I. Surface chemistry and ion binding properties, Carbon 40 (2002) 1493–1505.
[43] L.J. Kennedy, J.J. Vijaya, K. Kayalvizhi, G. Sekaran, Adsorption of phenol from aqueous solutions using mesoporous carbon prepared by two-stage process, Chem. Eng. J. 132 (2007) 279–287.
[44] M.A. Montes-Morán, D. Suárez, J.A. Menéndez, E. Fuente, On the nature of basic sites on carbon surfaces: An overview, Carbon 42 (2004) 1219–1225.
[45] R. Baccar, J. Bouzid, M. Feki, A. Montiel, Preparation of activated carbon from Tunisian olive-waste cakes and its application for adsorption of heavy metal ions, J. Hazard. Mater. 162 (2009) 1522–1529.
[46] L.B. Khalil, B.S. Girgis, Adsorption of PNP on activated carbon prepared from phosphoric acid treated apricot stone shells, Ads. Sci. Technol. 12 (1995) 79–92.
[47] A.A.M. Daifullah, B.S. Girgis, H.M.H. Gad, A study of the factors affecting the removal of humic acid by activated carbon prepared from biomass material, Colloids and Surfaces A: Physicochem. Eng. Aspects 235 (2004) 1–10.
[48] D. Doulia, C. Leodopoulos, K. Gimouhopoulos, F. Rigas, Adsorption of humic acid on acid-activated Greek bentonite, J. Colloid Interface Sci. 340 (2009) 131–141.
[49] S. Wang, Z.H. Zhu, Humic acid adsorption on fly ash and its derived unburned carbon, J. Colloid Interf. Sci. 315 (2007) 41–46.
[50] X. Peng, Z. Luan, H. Zhang, Montmorillonite-Cu(II)/Fe(III) oxides magnetic material as adsorbent for removal of humic acid and its thermal regeneration, Chemosphere 63 (2006) 300–306.
[51] V.K. Garg, R. Kumar, R. Gupta, Removal of malachite green dye from aqueous solution by adsorption using agro-industry waste: A case study of Prosopis cineraria, J. Dyes Pig. 62 (2004) 1–10.
[52] S. Deng, R. Bai, Adsorption and desorption of humic acid on aminated polyacrylonitrile fibers, J. Colloid Interface Sci. 280 (2004) 36–43.
[53] W.S. Wan Ngah, M.A.K.M. Hanafiah, S.S. Yong, Adsorption of humic acid from aqueous solutions on crosslinked chitosan–epichlorohydrin beads: Kinetics and isotherm studies, Colloid. Surf. B: Biointerfaces 65 (2008) 18–24.
[54] L. Monser, N. Adhoum, Tartrazine modified activated carbon for the removal of Pb(II), Cd(II) and Cr(III), J. Hazard. Mater. 16 (2009) 263–269.
[55] B. Nasr, B. Hedi, G. Abdellatif, M. Rodrigo, Purification of wet-process phosphoric acid by hydrogen peroxide oxidation, activated carbon adsorption and electrooxidation, Chem. Eng. Technol. 28 (2005) 193–198.
[56] A. Silem, A. Boualia, A. Mellah, R. Kada, Quantitative and qualitative analysis of organic matter contained in industrial phosphoric acid, Can. J. Appl. Spectrosc. 36 (1991) 94–97.